International Journal of Astrobiology 8 (1): 3–8 (2009) Printed in the United Kingdom
doi:10.1017/S1473550408004382

Glittery clouds in exoplanetary atmospheres?

Ch. Helling[1] and F.J.M. Rietmeijer[2]

[1]*SUPA, School of Physics and Astronomy, University of St Andrews, North Haugh, St Andrews, KY16 9SS, UK*
e-mail: ch80@st-and.ac.uk
[2]*Department of Earth and Planetary Sciences, MSC03-2040, University of New Mexico, Albuquerque, NM 87131-0001, USA*

Abstract: Cloud formation modelling has entered astrophysics as a new field of research for planetary and brown dwarf atmospheres. Clouds are a chemically and physically very active component of an atmosphere since they determine the remaining gas phase and change the object's albedo depending on their material composition. The grains can also provide a surface where the molecular constituents for life can be physisorbed for possible pre-biotic evolution. This paper summarizes our model for the kinetic formation of dirty dust grains which make up the atmospheric clouds of extraterrestrial giant gas planets. We include seed formation, surface growth and evaporation, the gravitational settling that influences the dust formation, element depletion that determines the remaining gas phase abundances, and convective overshooting that is needed for a dust model to be applicable to hydrostatic atmosphere simulations. We demonstrate the evolution of the material composition of the cloud itself and the distribution of the grain sizes in the cloud layer, exemplary for a giant gas planet parameter combinations ($T_{\rm eff}$, log g). In general, substellar clouds are composed of small, dirty grains with a high silicate content at the cloud deck. They grow in size and gradually purify to iron/corundum grains when they move into denser and hotter atmospheric regions. Comparing these results with experimental data from condensation experiments leads to the conclusion that cloud grains that gravitationally settle in the atmosphere of a giant planet can easily change their lattice structure from the disordered amorphous state they are forming in, into the ordered lattice of a crystal.

Received 1 October 2008, accepted 18 November 2008, first published online 21 January 2009

Key words: Astrochemistry, Methods: Numerical, Stars: Atmospheres, stars: low-mass, brown dwarfs, Planets: Atmospheres.

Introduction

Planets are covered by atmospheres which have a complex gas phase and cloud chemistry, which under certain circumstance might breed life. Planets form as by-products of star formation, and depending on their size, they can have effective temperatures comparable to Earth, or much hotter than Jupiter. Hence, the clouds forming in extraterrestrial planets can be as diverse as their fundamental parameters are: the clouds can be composed of liquids such as water or of solid dust grains, all determining the thermal structure of the atmosphere by their ability to absorb radiation. Recent support for this idea came from observations by Richardon *et al*. (2007) and Pont *et al*. (2008), who suggested that high-altitude small grains exist in giant gas planets based on *Spitzer* and *HST* observations, respectively. Such cloud grains might serve as seeds for microbes to develop under rather extreme conditions, since the grains provide a surface where the molecular constituents for life can be physisorbed for possible pre-biotic evolution.

History and evolution of a cloud's dust grain

The cloud formation process involves a variety of microphysical and macrophysical processes leading to the formation of dust grains with a variety of sizes. These processes act at different time and length scales, as is known from the formation of thunder clouds in the terrestrial atmosphere. The main difference between the Earth and extraterrestrial planets is that for extraterrestrial planets we cannot *a priori* assume that there are aerosol-like particles which act as seeds for a subsequent surface reaction leading to the formation of water droplets. Hence, the formation of a grain has to start with the formation of a seed particle (*nucleation*). Nucleation can only takes place if the gas is supersaturated, hence supercooled, regarding a certain solid. In our case, we consider the formation of TiO_2 seed particles which form by a homogeneous, stationary nucleation process during which the next large cluster is formed by adding another TiO_2 monomer. Note that such a homogeneous nucleation process is not always possible, namely, if the monomer is not present in the

gas phase, as in the case of Al_2O_3. However complex this chemical path from the gas phase to solid phase might be, the nucleation process is a sequence of gas–gas collisions. Once the seed particle is formed from the gas phase by a certain sequence of chemical reactions, many other solids are already thermally stable and can therefore form through chemical surface reactions. Hence, several solids will grow almost simultaneously (here TiO_2[s], SiO[s], SiO_2[s], Fe[s], FeO[s], Fe_2O_3[s], FeS[s], MgO[s], $MgSiO_3$[s], Mg_2SiO_4[s], Al_2O_3[s] and $CaTiO_3$[s]) by certain chemical surface reactions (here 60). The rate with which this reaction sequence contributes to the growth of a particular solid is determined by the abundance of a key molecule which is the lowest abundance molecule amongst the reactants (Helling & Woitke 2006). So far, there is no difference in the dust formation scenario compared with asymptotic giant branch stars which provide the only other place of efficient dust formation in the universe. However, giant gas planets and brown dwarfs have a very large surface gravity since they are very compact objects. A grain that forms in these atmospheres instantaneously starts to sink into the atmosphere under the pull of the object's gravity (Woitke & Helling 2003). The grain encounters a continuously increasing gas density which leads to a runaway process: the higher the gas density, the faster and bigger the grain grows, so the faster it falls into even higher-density regions. This process is stopped if the frictional force, which also increases with increasing density, balances the gravitational force pulling the grain, or if the grain evaporates in regions where the solids become thermally unstable. Once the grain evaporates, it elementally enriches these layers of evaporation but elementally depletes those layers through which it has fallen. The consequence is that the spectral features in a dust-forming atmosphere would be much shallower compared with a dust-hostile atmosphere. In principle, processes between existing particles can cause a further increase in the particle size (coagulation), a change in the lattice structure (annealing, solid diffusion, internal rearrangement) or a change in the charge state of the grains. These processes are not included in our dust formation model, but we discuss the implications of condensation experiments for the lattice structure (i.e. crystallinity) of the cloud particles.

The dust formation model

It seems appropriate to summarize the equations which were derived in order to model the formation of dirty dust grains by those processes outlined in the previous section, i.e. by nucleation, growth, gravitational settling (drift) including the evaporation process and element consumption. This system of equations is solved numerically in order to study the structure of a dust cloud as it may appear in giant gas planets.

We start by defining the dust moments $L_j(\vec{x}, t)$ (cm^j/g) as

$$\rho L_j(\vec{x}, t) = \int_{V_\ell}^{\infty} f(V, \vec{x}, t) V^{j/3}\, dV. \quad (1)$$

Here V_ℓ is the minimum volume of a large molecule ('cluster') to be counted as a dust grain and $f(V)$ (cm^{-6}) is the size distribution of the dirty dust grains which will make up the cloud. To allow the dust cloud model to be linked with a radiative transfer model, a plane–parallel quasi-static stellar atmosphere is considered where $\mathbf{v}_{\mathrm{gas}} = 0$. Hence, the dust component is stationary since hydrodynamic velocity is neglected. The reader is referred to Woitke & Helling (2003) and Helling & Woitke (2006) for the complete time-dependent dust cloud model and its derivation. Introducing a convective mixing on a time scale τ_{mix} we have derived the following equations for this case (see Woitke & Helling (2004, (7)))

$$-\frac{d}{dz}\left(\frac{\rho_d}{c_T} L_{j+1}\right) = \frac{1}{\xi_{lKn}}\left(-\frac{\rho L_j}{\tau_{\mathrm{mix}}} + V_\ell^{\,j/3} J_\star + \frac{j}{3}\chi^{\mathrm{net}} \rho L_{j-1}\right). \quad (2)$$

These are *the moment equations with respect to the total dust volume* for dirty grains and we use them for $j = 0, 1, 2$. As outlined in Woitke & Helling (2004, (9)), τ_{mix} is the time scale for mixing due to convective motions and overshoot which decreases rapidly above the convective layers with increasing height in the atmosphere. In order to treat the formation of dirty dust grains, we assume they are made of small solid islands. Another set of equations needs to be solved to allow the calculation of the individual solids' volumes (Helling & Woitke 2006). These are the third dust moment equations for all volume contributions providing one equation for each condensate s:

$$-\frac{d}{dz}\left(\frac{\rho_d}{c_T} L_4^s\right) = \frac{1}{\xi_{lKn}}\left(-\frac{\rho L_3^s}{\tau_{\mathrm{mix}}} + V_\ell^{\,s} J_\star + \chi^s_{\mathrm{net}} \rho L_2\right). \quad (3)$$

Equations (2) for $j \in \{0, 1, 2\}$ and (3) for $s \in \{1, 2, \ldots, S\}$ (S is the number of solid condensates taken into account) form a system of $(S+3)$ ordinary differential equations for the unknowns $\{L_1, L_2, L_3, L_4^s\}$. The source terms on the right-hand sides of (2) and (3) describe the effects of the nucleation, growth and evaporation of condensate s. Here $J_* = J(V_\ell) = f(V_\ell)(dV/dt)|_{V=Vl}$ (per second per cubic centimetre) is the stationary nucleation rate with V_ℓ^s (in cubic centimetres) is the volume occupied by condensate s in the seed particles when they enter the integration domain in size space. The nucleation rate is calculated from

$$J_* = \frac{n_x}{\tau} Z \exp\left[(N_* - 1)\ln S - \left(\frac{T_\Theta}{T}\right)\frac{(N_* - 1)}{(N_* - 1)^{1/3}}\right], \quad (4)$$

applying the modified classical nucleation theory of Gail *et al.* (1984). The seed growth time scale is $\tau^{-1} = n_x v_{\mathrm{rel},x} N_*^{2/3} A_0$ for a gaseous nucleation species x with a relative velocity v_{rel}. Here $T_\Theta = 4\pi a_0^2 \sigma / k$ with a_0 being the hypothetical monomer radius and with a value of the surface tension σ fitted to small cluster data based on quantum mechanical calculations of the cluster structures by Jeong *et al.* (2000).

The net growth velocity of condensate s, χ^s_{net} (in centimetres per second, negative for evaporation), is given by (Helling & Woitke (2006), (24))

$$\chi^s_{\mathrm{net}} = \sqrt[3]{36\pi} \sum_{r=1}^{R} \frac{\Delta V_r^s n_r^{\mathrm{key}} \mathrm{v}_r^{\mathrm{rel}} \alpha_r}{\mathrm{v}_r^{\mathrm{key}}} \left(1 - \frac{1}{S_r b^s_{\mathrm{surf}}}\right). \quad (5)$$

https://doi.org/10.1017/S1473550408004382 Published online by Cambridge University Press

Here, r is an index for the chemical surface reactions (see Table 1 in Helling *et al.* (2008)), ΔV_r^s is the volume increment of solid s by reaction r ($\Sigma\Delta V_r^s = \Delta V_r$), $n_r^{\rm key}$ is the particle density of the key reactant, $\nu_r^{\rm rel}$ is its thermal relative velocity and α_r is the sticking coefficient of reaction r; S_r is the reaction supersaturation ratio and $b_{\rm surf}^s = V_{\rm tot}/V_s$ is a b-factor which describes the probability of finding a surface of kind s on the total surface. Putting $b_{\rm surf}^s$ independent of V, we assume that all grains at a certain point in the atmosphere have the same surface and volume composition, i.e. the grain material is a homogeneous mix of islands of different kinds (for more details see Helling *et al.* (2008)).

The element conservation is expressed as follows and the equations are not affected by the drift motion of the dust grains,

$$\frac{n_{\langle \rm H\rangle}(\varepsilon_i^0 - \varepsilon_i)}{\tau_{\rm mix}} = \nu_{i,0} N_\ell J_\star + \sqrt[3]{36\pi}\rho L_2 \sum_{r=1}^{R} \frac{\nu_{i,s} n_r^{\rm key} v_r^{\rm rel} \alpha_r}{\nu_r^{\rm key}} \times \left(1 - \frac{1}{S_r b_{\rm surf}^s}\right), \quad (6)$$

where i enumerates the elements. Here N_ℓ is the number of monomers in the seed particles when they enter the size integration domain and $\nu_{i,0}$ is the stoichiometric coefficient of the seeds (TiO_2 seeds: 1 for i=Ti and 2 for i=O); $\nu_{i,s}$ is the stoichiometric coefficient of element i in solid material s. These element conservation equations (6) provide algebraic auxiliary conditions for the ordinary differential equation (ODE) system (2) and (3) in the static stationary case, i.e. one first has to solve the system of nonlinear algebraic equations (6) for ε_i at given $\{L_2, L_4^s\}$ (the dust volume composition $b_{\rm surf}^s$ is known from L_4^s) before the right-hand side of the ODEs can be calculated. Since J_*, $n_r^{\rm key}$ and, in particular, S_r, however, depend strongly on ε_i, this requires a iterative procedure.

The dust cloud structure

The study of various cloud details is possible after the solution of the equations given in the previous section for a given temperature T, gas pressure p and convective velocity $v_{\rm conv}$. Figure 1 shows, for instance, the nucleation rate J_* (solid curve, second panel), which demonstrates that the seed formation takes place in the upper cloud region. Hence, each dust grain found at lower altitudes then this must have rained in from above. Figure 1 also depicts the net growth velocity, $\chi_{\rm net} = \sum \chi_{\rm net}^s$ (dashed curve, second panel), which is approximately zero in the region of efficient nucleation. Dust growth by chemical surface reactions becomes the dominating dust formation process where nucleation becomes inefficient in the model case shown here. Figure 1 shows further that $\chi_{\rm net}$ has various minima and maxima which are indicative of evaporation and growth processes of certain dust compounds. Note that the dust compounds are in extreme phase non-equilibrium in the nucleation region and that only low-temperature condensates will reach approximate phase equilibrium in a limited region of the dust cloud. High-temperate condensates

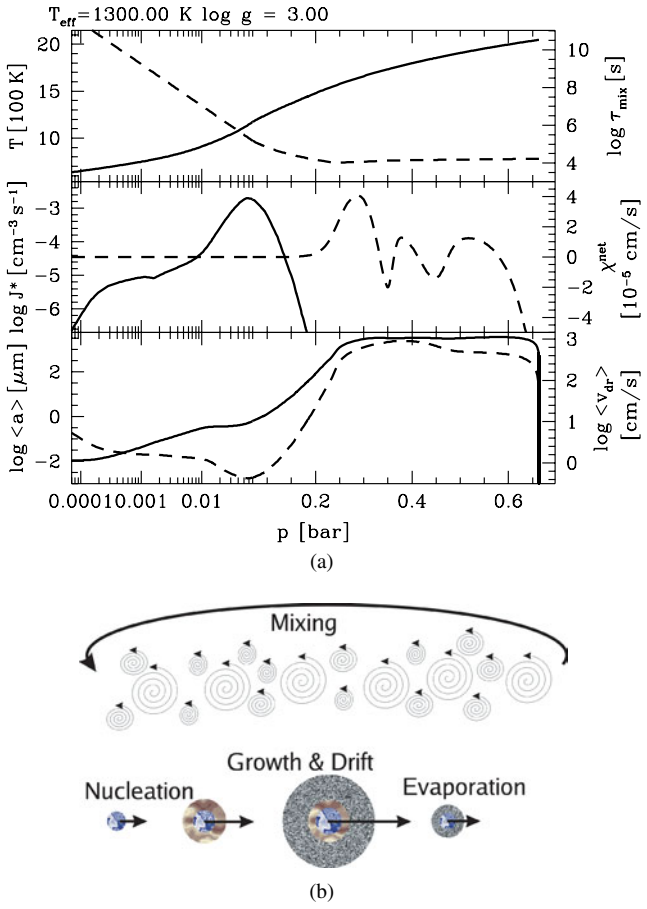

Fig. 1. Dust cloud structure (a) and schematic of the formation path (b) of a dust grain, an ensemble of which forms the dust clouds in substellar objects. In the first panel, the solid curve shows the local temperate T (in Kelvin) and the dashed curve shows the mixing time scale $\tau_{\rm mix}$ (in seconds); in the second panel, the solid curve shows the nucleation rate J_* (in cubic centimetres per second) and the dashed curve shows the net growth velocity $\chi_{\rm net} = \sum \chi_{\rm net}^s$ (in centimetres per second); in the third panel, the solid curve shows the mean grain size $\langle a\rangle = \sqrt[3]{3/(4\pi)} L_1/L_0$ ($\times 10^{-4}$ cm) and the dashed curve shows the drift velocity $\langle v_{\rm dr}\rangle = \sqrt{\pi} g \rho_d \langle a\rangle / (2\rho c_T)$ (in centimetres per second).

such as TiO_2[s], Al_2O_3[s] and $CaTiO_3$[s] never reach phase equilibrium (Helling *et al.* (2008)).

The mean grain size can be derived from the dust moments as $\langle a\rangle = = \sqrt[3]{3/(4\pi)} L_1/L_0$ (Fig. 1, solid curve, third panel) shows that small dust grains populate the upper cloud but large grains should be found at the cloud base. It is interesting to compare this with the material composition of the cloud in substellar atmospheres (Fig. 2) which demonstrates that the small grains populating the cloud deck are made up of a large fraction of silicates ($MgSiO_3$[s], Mg_2SiO_4[s], SiO_2[s]) with impurities of oxides (MgO[s], FeO[s]) and iron (Fe[s]). Figure 2 shows that the grains are not made of only one material, but the grain volume is made up of a variety of thermally stable solids which form under phase non-equilibrium temperatures. A comparison with Fig. 1 shows furthermore that the grains purify as they grow and that the large grains at the

https://doi.org/10.1017/S1473550408004382 Published online by Cambridge University Press

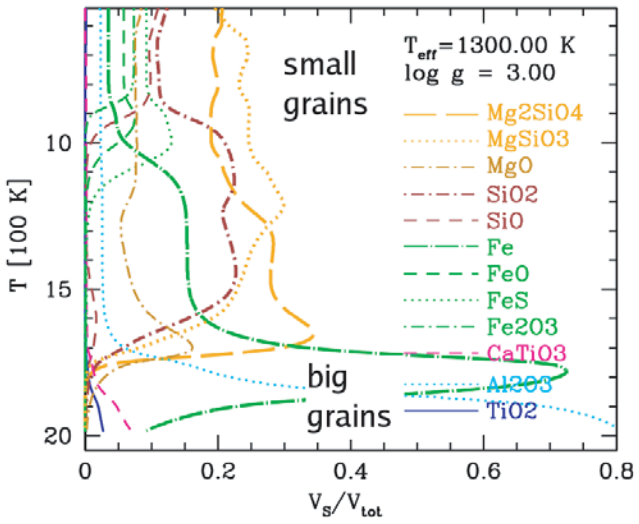

Fig. 2. The material composition of clouds inside the atmosphere of a giant gas planet: small silicate grains with iron and oxide impurities populate the upper cloud, and large iron grains with some corundum impurities populate the cloud base.

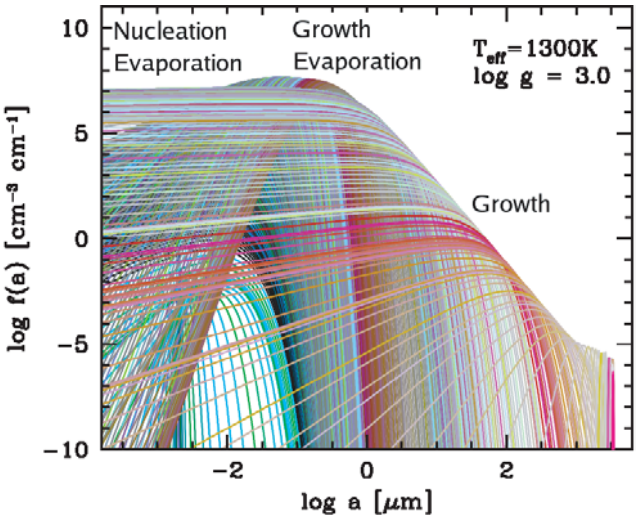

Fig. 3. Grain size distribution functions throughout the dust cloud layer in a giant gas planet.

cloud base are almost entirely composed of solid iron. Hence, the grains do change their material composition as they fall inwards since the local temperature changes cause the materials to become thermally instable, and hence to evaporate. Thermally more stable materials such as Fe[s] and Al_2O_3[s] then make up most of the grain volume in the warmest cloud layers.

The grain size distribution in the cloud layer

The grain size distribution, $f(a)$, is not a direct result of our model since we are solving conservation equations for the moments of the size distribution function. The size distribution $f(a)$ can, however, be derived if a certain number of dust moments $L_j(V)$ is known. In Helling *et al.* (2008, Appendix A) we demonstrated how the grain size distribution can be deduced by using the idea of Dominik *et al.* (1986) and Gauger *et al.* (1990) who derived $f(a)$ with the grain radius space (a) instead of the grain volume space (V). For now, we use a simple representation of $f(a)$ as an exponential function such that

$$f(a) = a^B \exp(A - Ca), \tag{7}$$

which, for positive coefficients A, B and C, is strictly positive with a maximum at B/C. Since there are only three coefficients in (7) we determine them from K_1, K_2 and K_3 with

$$K_j = \int_{a_\ell}^{\infty} f(a) a^j \, da = \left(\frac{3}{4\pi}\right)^{j/3} \rho L_j(V).$$

Figure 3 shows the resulting grain size distributions $f(a)_i$ for $i = 1, \ldots \approx 100$ throughout the cloud layer. The grain size distribution functions are delta functions if nucleation dominates (at around 10^{-3} μm in Fig. 3). The number of dust particles still increases but they also start to grow in size which causes $f(a)$ to gain height and simultaneously to move to the right in the grain size space. Moving further inwards towards higher temperature causes the evaporation of solids which causes the grain size distribution to spread over a large grain size interval and the number of grains per size interval to decrease. Some cloud layers close to the regime of complete evaporation again exhibit a delta peak like $f(a)$ at large grain sizes (around $10^{3.5}$ μm) since all small particles have already been destroyed.

Glittery or not?

All models of vapour phase condensation in astronomical environments have their origins in our attempts to explain the objects in the Solar System, in particular the most primitive asteroids that are represented by only a few carbonaceous chondrite meteorites. All solids in the Solar System, and in extra-Solar nebulae around other stars, initially condensed from a cooling nebula. Thus, experimental verification of the Solar nebula's bulk composition (e.g. Anders & Grevesse (1989), Lodders & Fegley (2006) and many others) was the key to unlocking cosmochemistry and astronomy research.

Vapour phase condensation can be addressed as a thermodynamic equilibrium process, or as a kinetically controlled process leading to metastable condensates with non-equilibrium compositions. The low-vacuum conditions in space environments favour direct vapour to solid processes, which is also the case in brown dwarfs and giant gas planets. Any condensate formation (solid or liquid) requires that a condensing species be supersaturated with respect to its equilibrium concentration at given pressure and temperature. In thermodynamic equilibrium, i.e. phase equilibrium, nucleation cannot happen, and hence no subsequent growth can occur that would otherwise require less activation energy and supersaturation than the nucleation process. Still, the conditions in large volumes of quiescent, gradually cooling gases

https://doi.org/10.1017/S1473550408004382 Published online by Cambridge University Press

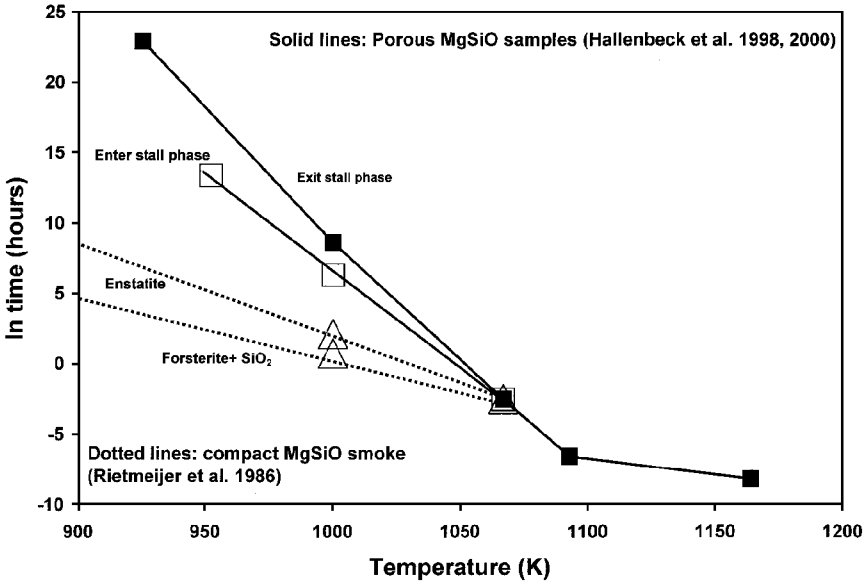

Fig. 4. The time–temperature relation of stall rates for a condensed porous MgSiO smoke for the formation of crystalline silicates. The post-stall phase is characterized by changes in the IR spectra that indicate the crystallization of forsterite (Mg_2SiO_4), tridymite (a high-temperature SiO_2 polymorph) and enstatite ($MgSiO_3$). Transmission electron microscopy studies confirmed that the amorphous condensate grains grew into amorphous clumps and the crystallization of these (Rietmeijer *et al.* (2002a)). Starting with a compact clump of vapour-condensed amorphous MgSiO material, thermal processing will bypass the stall phase with crystallization happening rapidly (Rietmeijer *et al.* 1986).

after the seed formation might then favour the appearance of an orderly sequence of well-ordered, stoichiometric solids, i.e. minerals, as a function of decreasing equilibrium temperatures, including chemically complex minerals such as the high-temperature minerals gehlenite, $Ca_2Al_2SiO_7$, and spinel, $MgAl_2O_4$ (Grossman & Larimer 1974). These condensed minerals are stable phases that will resist modification when the gas conditions change and they will be long-lived.

Thermodynamic equilibrium makes it possible to calculate condensation sequences while varying a parameter of choice such as the C/O ratio of the gas phase. However, it is more likely that the vapour phase condensation process in natural environments will be kinetically controlled and thus will be a non-equilibrium process. If this is so, the process becomes chaotic and all predictability is lost. However, when vapour phase condensation occurs far from thermodynamic equilibrium, De (1979) suggested the emergence of dissipative structures that Prigogine (1978) defined as a new state of matter where extreme disorder becomes a metastable state of matter. Thus, extreme non-equilibrium condensation becomes predictable but it will not produce minerals. When given time and opportunity, extreme non-equilibrium condensates may reach a state of thermodynamic equilibrium but the ultimate mineral assemblages will be unpredictable. However, they will have formed at temperatures well below their thermodynamic stability fields. For example, forsterite olivine (Mg_2SiO_4) is a high-temperature (1450 K) equilibrium Solar nebula condensate but rapidly crystallizes in non-equilibrium, amorphous magnesiosilica condensates produced at much lower temperatures (1038 K) (Rietmeijer *et al.* 2002a).

Laboratory vapour phase condensation experiments have successfully defined the nature of these extreme non-equilibrium condensates. They are highly disordered, amorphous solids ranging from around 2 nm to about 25 nm in diameter with unique deep metastable eutectic metal oxide/SiO ratios (M = Mg, Fe, Ca, Al and combinations thereof) (Nuth *et al.* 1999, 2000; Rietmeijer *et al.* 2002b, 2008). These nanometer-scale condensate grains from porous three-dimensional structures of interconnected necklaces of individual grains are known as 'smokes'. The metastable condensates that are entirely different from equilibrium minerals are highly responsive to post-condensation changes in their environment, such as thermal processing falling into a denser and warmer environment (cf. Fig. 1). Using infrared (IR) spectroscopy Hallenbeck *et al.* (1998, 2000) monitored the controlled changes in amorphous magnesiosilica smokes as a function of time and temperature to track the formation of crystallization and formation of forsterite, enstatite pyroxene ($MgSiO_3$) and tridymite (SiO_2). Following an initial period of subtle IR changes, continued heating did not show further structural or chemical changes. The process appeared to have stalled in its development. Continued heating produced evidence of the formation of these three minerals during the so-called post-stall phase. Rietmeijer *et al.* (2002a) showed that during the stall phase the porous smoke of nanometer-scale condensates was collapsing into initially small 50 nm massive volumes when individual condensate grains had fused and were chemically homogenized. These massive clumps were the sites of crystallization of these minerals. Hallenbeck *et al.* (2000) developed reaction rate equations for the onset of the stall phase and when the samples exited the stall phase. These equations

https://doi.org/10.1017/S1473550408004382 Published online by Cambridge University Press

predict when crystallization began in the 50 nm clumps. Similar annealing studies of magnesiosilica smokes (Fabian *et al*. 2000; Thompson & Tang 2001) found evidence for a stall phase because their initial condensate grains were on average larger than 50 nm. Thus, in their experiments there was no necessity to first evolve the minimum size amorphous clumps required for crystallization. The rate equations from Hallenbeck *et al*. (2000) will then be able to constrain whether crystallization will be able to occur in a circumstellar nebula wherein grains with at least this minimum size must be present. We advise caution in that the currently available data for magnesiosilica compositions cannot be extrapolated to condensate grains of other compositions. Hallenbeck *et al*. (1998) observed that crystallization in amorphous ferrosilica smokes would take much longer than in amorphous magnesiosilica smokes when the original condensates grains in both were much less than about 50 nm.

Figure 4 demonstrates the time–temperature relation of stall rates according to Hallenbeck *et al*. (2000) for a porous sample (smoke) of condensed grains, that is, the beginning stall phase (open squares) and the beginning of the post-stall phase (solid squares) when crystalline silicates were formed. The open triangles show the time–temperature relation for crystallization in a condensed sample that, because of its compact nature, did not require a stall phase to create the conditions necessary for crystallization of the minerals indicated in the figure. Figure 4 shows clearly that an already existing solid (such as the grains making up the dust cloud) does not need to go through a stall phase but that the formation of silicate crystals occurs much faster as a function of temperature than if the crystals would need to form directly from the gas phase. This means that the silicate grains that populate the atmosphere at temperatures between around 1200 and 1800 K would almost instantaneously crystallize while falling from above into these regions (cf. Fig. 1(b)). It might be possible that during continuing growth in a cooling gas crystalline grains will be covered by an amorphous mantle of condensed materials. The far smaller dust grains which are made of amorphous solids at the top of the cloud would need to go through a stall phase, hence they would need time and energy to rearrange their lattice structure.

Conclusion

The formation of dust clouds can be described as a sequence of physiochemical non-equilibrium processes: nucleation (seed formation), growth and evaporation (surface reactions), element depletion, gravitational settling (rain) and element replenishment by convective overshoot. The resulting cloud structure reflects these processes by, for instance, very narrow grain size distributions at the cloud top where seed formation dominates the dust formation processes. These seeds fall into the atmosphere and become covered by a variety of species such as oxides and silicates until they disappear from the grain because they evaporate. The cloud centre shows vivid growth processes which cause the grain size distribution to broaden considerably. The biggest grains are found at the cloud base which are made of iron and some inclusions of Al_2O_3[s] and TiO_2[s]. Laboratory experiment suggest that these grains which fall from a cooler into warmer atmospheric layers do rearrange their lattice structures from the disordered amorphous state in which they are forming into the ordered crystalline state. One consequence is the change of their optical properties which might make them more glittery than before.

References

Anders, E. & Grevesse, N. (1989). *Geochim. Cosmochim. Acta* **53**, 197.

De, B.R. (1979). Disequilibrium condensation environments in space: A frontier in thermodynamics. *Astrophys. Space Sci*. **65**, 191–198.

Dominik, C., Gail, H.-P. & Sedlmay, E. (1986). *Astron. Astrophys*. **223**, 227.

Fabian, D., Jäger, C., Henning, Th., Dorschner, J. & Mutschke, H. (2000). *Astron. Astrophys*. **364**, 282.

Gail, H.P., Keller, R. & Sedlmayr, E. (1984). *Astron. Astrophys*. **133**, 320.

Gauger, A., Sedlmayr, E. & Gail, H.-P. (1990). *Astron. Astrophys*. **235**, 345.

Grossman, L. & Larimer, J.W. (1974). *Geophys. Space Phys*. **1**, 71.

Hallenbeck, S.L., Nuth, J.A. III & Daukantes, P.L. (1998). *Icarus* **131**, 198.

Hallenbeck, S.L., Nuth, J.A. III & Nelson, R.A. (2000). *Astrophys. J*. **535**, 247.

Helling, Ch. & Woitke, P. (2006). *Astron. Astrophys*. **455**, 325.

Helling, Ch., Woitke, P. & Thi, W.-F. (2008). *Astron. Astrophys*. **485**, 547.

Jeong, K.S., Chang, C., Sedlmayr, E. & Sülzle, D. (2000). *J. Phys. B: At. Mol. Opt. Phys*. **33**, 3417.

Lodders, K. & Fegley, B. (2006). In *Astrophysics Update* 2, ed. J.W. Mason, Springer/Praxis Publ. Ltd., Chichester, UK.

Nuth, J.A. III, Hallenbeck, S.L. & Rietmeijer, F.J.M. (1999). Interstellar and interplanetary grains, Recent developments and new opportunities for experimental chemistry. In *Laboratory Astrophysics and Space Research*, eds Ehrenfreund, P., Krafft, K., Kochan, H. & Pirronello, V., pp. 143–182. Kluwer Acad. Publ., Dordrecht.

Nuth, J.A. III, Rietmeijer, F.J.M., Hallenbeck, S.L., Withey, P.A. & Ferguson, F. (2000). Nucleation, growth, annealing and coagulation of refractory oxides and metals: Recent experimental progress and applications to astrophysical systems. In *Thermal Emission Spectroscopy and Analysis of Dust, Disks and Regoliths*, eds Sitko, M.L. & Lynch, D.K., pp. 313–332. Astron. Soc. Pacific Conf. Series 196.

Prigogine, I. (1978). *Science* **201**, 777–785.

Pont, F., Knutson, H., Gilliland, R.L., Moutou, C. & Carbonneau, D. (2008). *Mon. Not. R. Astron. Soc*. **385**(1), 109.

Richardson, L.J., Deming, D., Horning, K., Seager, S. & Harrington, J. (2007). *Nature* **445**, 892.

Rietmeijer, F.J.M., Nuth, J.A. & Mackinnon, I.D.R. (1986). *Icarus* **65**, 211.

Rietmeijer, F.J.M., Pun, A., Kimura, Y. & Nuth, J.A. III (2008). *Icarus* **195**, 493.

Rietmeijer, F.J.M., Hallenbeck, S.L., Nuth, J.A. III & Karner, J.M. (2002a). *Icarus* **156**, 269–286.

Rietmeijer, F.J.M., Nuth, J.A. III, Karner, J.M. & Hallenbeck, S.L. (2002b). *Phys. Chem. Chem. Phys*. **4**, 546.

Thompson, S.P. & Tang, C.C. (2001). *Astron. Astrophys*. **368**, 721.

Woitke, P. & Helling, Ch. (2003). *Astron. Astrophys*. **399**, 297.

Woitke, P. & Helling, Ch. (2004). *Astronomy & Astrophysics*. **414**, p. 335.

https://doi.org/10.1017/S1473550408004382 Published online by Cambridge University Press